

Imaging features of spinal atypical teratoid rhabdoid tumors in children

Hui-Ying Wu, MS^a, Wen-Biao Xu, BS^{a,*}, Lian-Wei Lu, MS^a, He-Hong Li, MD^a, Jin-Sheng Tian, MS^a, Jian-Ming Li, BS^a, Zheng-Rong Chen, MS^b

Abstract

This study aims to analyze and summarize the imaging features of spinal atypical teratoid/rhabdoid tumors (AT/RT) in children.

Imaging features in 8 children with spinal AT/RT confirmed by surgical pathology were retrospectively analyzed. All patients had undergone total spine 3.0T magnetic resonance imaging (MRI) and 64-slice spiral computed tomography (CT). Among these 8 patients, head MR non-enhanced and spinal enhanced scanning was applied to 5 patients, while CT examination was applied to 3 patients.

All 8 patients were characterized by cauda equina syndrome. The lesions of 7 patients were in the thoracolumbar spinal junction, while the lesion of the remaining patient was in the lumbar spine. Furthermore, among these patients, the lesions of 5 patients were limited to the intraspinal canal (1 lesion in the epidural space, and 4 lesions in the subdural space), while the lesions of 3 patients invaded the paravertebra (2 lesions in the epidural space and 1 lesion in the subdural space). Three or more spinal segments were invaded by tumors in 7 patients, while sacral canal was affected in 5 patients. All 8 patients experienced bleeding in the tumors. Enhanced MRI revealed meningeal enhancement in 6 patients, and bilateral nerve root enhancement in 4 patients. The masses in 3 patients brought damages to the intervertebral foramen or sacral pore. The lesion of 1 patient was featured by skip growth. One patient had total spinal metastasis and 3 had hydrocephalus. The masses in 2 patients had a slightly low density when detected by CT, and enhanced scanning revealed a mild to moderate enhancement.

Spinal AR/TR had the following characteristics: children were characterized by cauda equina syndrome; the mass that invaded the thoracolumbar spinal junction and the extramedullary space of multiple segments grew along the spinal longitudinal axis; bleeding mass was revealed in MRI imaging; meninges, nerve root, and sacral canal metastases occurred. The gold standard for the definite diagnosis of AT/RT is biopsy combined with immunohistochemistry.

Abbreviations: AT/RT = atypical teratoid/rhabdoid tumors, CNS = central nervous system, CT = computed tomography, EERT = extrarenal extracranial rhabdoid tumor, EMA = epithelial membrane antigen, FOV = field of view, GFAP = glial fibrillary acidic protein, INI-1 = integrase interaction molecules, LMD = leptomeningeal dissemination, MRI = magnetic resonance imaging, MRTK = malignant rhabdoid tumor of the kidney, PNET = primitive neuroectodermal tumor, RT = rhabdoid tumor, SMA = smooth muscle actin, TE = echo delay time, TR = repetition time, WHO = World Health Organization.

Keywords: children, computed tomography, malignant rhabdoid tumor, magnetic resonance imaging, spine

1. Introduction

Atypical teratoid/rhabdoid tumor (AT/RT) is a rare and aggressive type of embryonal tumor of the central nervous system (CNS) occurring in childhood. AT/RT represent brain tumor in early children, which is the most common CNS primary

malignant tumor in children <6 months old.^[1–4] In recent years, reports on craniocerebral AT/RT have gradually increased in China and foreign countries.^[5–7] It composes predominantly of poorly differentiated elements frequently with rhabdoid cells and characterized by biallelic loss of function alterations of SMARCB1, which encodes the hSNF5/BAF47/INI-1 subunit of the SWI/SNF chromatin remodeling complex, and more rarely SMAR-CA4, which encodes the SWI/SNF subunit BRG1. INI-1 is located on chromosome 22q11.23, loss of immunohistochemical expression of INI-1 protein is sensitive and specific to diagnosis of malignant rhabdoid tumors.^[8,9]

There is presently no standardized treatment regimen for AT/RT. Historically, AT/RT has been treated with surgical resection alone. However, more recent studies have demonstrated similar benefits of adjuvant chemotherapy.^[10,11] Complete surgical resection can often be challenging due to young age at diagnosis and tumor location in the brain. In addition, most physicians avoid radiation in very young children due to severe neurocognitive late effects. Intensive chemotherapy regimens are currently under study, but no standard chemotherapy regimen exists for these patients.^[3] Despite prolonged survival, overall mortality exceeds 60%, and most affected children suffer from long-term neurocognitive and developmental impairments.^[12] Retrospective data highlight the highly malignant nature of this disease with observed survival estimates at 1 year of $\leq 50\%$.^[13,14]

Editor: Surinder Kumar.

All authors have contributed significantly to the manuscript and declare that the work is original and has not been submitted or published elsewhere. None of the authors have any financial disclosure or conflict of interest.

^a Department of Imaging Center, ^b Department of Pathology, Guangzhou Women and Children's Medical Center, Guangzhou, Guangdong, China.

* Correspondence: Wen-Biao Xu, Department of Imaging Center, Guangzhou Women and Children's Medical Center, No 9 of Jinsui road, Zhujiang New Town Guangzhou, 510000, Guangdong province, China (e-mail: xuwenbiao1903@163.com).

Copyright © 2018 the Author(s). Published by Wolters Kluwer Health, Inc. This is an open access article distributed under the terms of the Creative Commons Attribution-Non Commercial-No Derivatives License 4.0 (CCBY-NC-ND), where it is permissible to download and share the work provided it is properly cited. The work cannot be changed in any way or used commercially without permission from the journal.

Medicine (2018) 97:52(e13808)

Received: 16 August 2018 / Accepted: 28 November 2018

<http://dx.doi.org/10.1097/MD.0000000000013808>

However, all these studies mainly focused on the description and summarization of the clinical features of intracranial tumors, and few reports on AT/RT focused on imaging features of the spine.^[15–17] Therefore, the imaging and clinical data of 8 children with spinal AT/RT confirmed by surgical pathology were collected and analyzed. The investigators summarized the features of spinal AT/RT, to improve the diagnosis accuracy and reduce misdiagnosis.

2. Materials and methods

2.1. Clinical data

The study is a retrospective cohort research. Patients enrolled in the study were from South China and were diagnosed in Guangzhou Women and Children's medical center, which is the largest children's hospital in south China. The range of spinal AT/RT imaging and clinical data was from January 2008 to April 2018.

The inclusion criteria were pathological diagnosis of spinal cord AT/RT and primary location at spinal cord. The exclusion criteria were intracranial masses were significantly larger than those in spinal cord; spinal cord lesions were found after intracranial AT/RT treatment.

Clinical data including age (onset of the symptoms), sex, clinical symptoms, neurological examination, symptoms till the moment of the spinal MRI scan and treatment, were summarized and analyzed.

The present study was approved by the Ethics Committee of our hospital. An informed consent was signed by the guardians of all children before the examination.

2.2. Examination methods

Before the computed tomography (CT) and magnetic resonance imaging (MRI) examinations, all children fasted for 3 to 4 hours, and orally took chloral hydrate (0.5 mL/kg) for sedation. Then, the examination was performed after the children slept.

Eight children underwent whole spine non-enhanced and enhanced MRI scans. The Siemens Skyra 3.0T Germany AG Erlangen, superconducting MRI system was used for the MRI examination. The scanning of the spinal cross-section and sagittal section was conventionally performed in all children, and coronal scanning was performed in part of these children. The contrast agent was Gd-DTPA, and the dose was 0.2 mL/kg. The scanning parameters were as follows: T1WI: repetition time (TR) was 600 ms, and echo delay time (TE) was 8.8 ms; T2WI: TR was 3500 ms, and TE was 109 ms; the thickness of the scanning slice was 3 mm, and the gap between slices was 3 mm; the field of view (FOV) was 33×33 mm.

Five children underwent head non-enhanced and enhanced MRI scans, and the scanning instrument was *ibid*. The scans of the cross-section, coronal section, and sagittal section were conventionally performed. The scanning parameters were as follows: T1WI: TR was 500 ms, and TE was 10 ms; T2WI: TR was 4000 ms, and TE was 100 ms; the thickness of the scanning slice was 5 mm, and the gap was 1 mm; the FOV was 240×240 mm.

One child underwent total abdominal CT non-enhanced and enhanced examinations, 1 child underwent sacrococcygeal CT non-enhanced and enhanced examinations, and 2 children underwent craniocerebral CT non-enhanced and enhanced examinations. The Toshiba Aquilion 64-slice spiral CT was used for the upper abdominal and craniocerebral CT examina-

tions. The scanning parameters were as follows: tube voltage was 120 kV; tube current was 200 mA (head) and 70 mA (upper abdomen). The upper abdominal enhanced scan was performed with iohexol or iopromide, and the dose was 1.5 mL/kg.

2.3. Image analysis

The following imaging findings from the MRI and CT were observed by one chief radiologist and one deputy chief radiologist: lesion location (scope of involvement, spinal segment), shape, size, maximum diameter plane, signal (density), bleeding, enhancement characteristics, intracranial manifestation, invasion (surrounding and/or sacral invasion), and metastasis.

The results were agreed upon by the 2 radiologist.

2.4. Pathological biopsy and immunohistochemistry

Seven patients underwent mass resection and 1 patient underwent biopsy. All the specimens were used for pathological examination (gross and microscope) and immunohistochemistry (INI-1, GFAP, Ki-67, and EMA).

3. Results

3.1. Clinical data

Eight patients confirmed by pathology were retrospectively analyzed. Among these 8 children, 3 children were boys and 5 were girls (male:female = 3:5). The age (onset of the symptoms) of these children ranged within 2 to 5 years old, with a mean age of 3 ± 0.5 years old.

The clinical symptoms of these children mainly manifested as cauda equina syndrome (8/8), with the most obvious changes in the lower extremities. Among these 8 children, weakness in the lower limbs and reluctance to walk were found in 5 children (5/8), while pains in the lower limbs were found in 3 children (3/8). Furthermore, urinary retention was found in 2 children (2/8), urinary incontinence was found in 1 child (1/8), headache was found in 2 children (2/8), fever was found in 1 child (1/8), and vomiting was found in 1 child (1/8). Neurological examination revealed that all 8 children had decreased lower limbs myodynamia (from grade 0 to grade 4) and had no other neurological positive signs.

The course of the disease varied within 5 to 90 days, and the mean duration from the onset of symptoms to the moment of the spinal MRI scan was 30.6 ± 22.2 days. All children were hospitalized for examination after onset of symptoms without special treatment.

3.2. Imaging manifestation

3.2.1. Scope of involvement of the tumor and the location.

According to the presence of soft tissue masses in the paraspinal region, tumors were divided into 2 types: Type I: this tumor is confined to the spinal canal. A total of 5 children (cases 1–5) had this type of tumor, accounting for 62.5% (the tumor was in the epidural space in one child, while the tumor was in the subdural space in 4 children). Type II: These tumors invaded the paravertebral tissue and vertebral canal (the tumor was in the right paravertebral region in 2 children, while the tumor was in the left sacrococcygeal region in 1 child). In 3 children (cases 6–8), tumor origin could not be distinguished, accounting for 37.5%. Among these children, the tumor affected the epidural space in 2

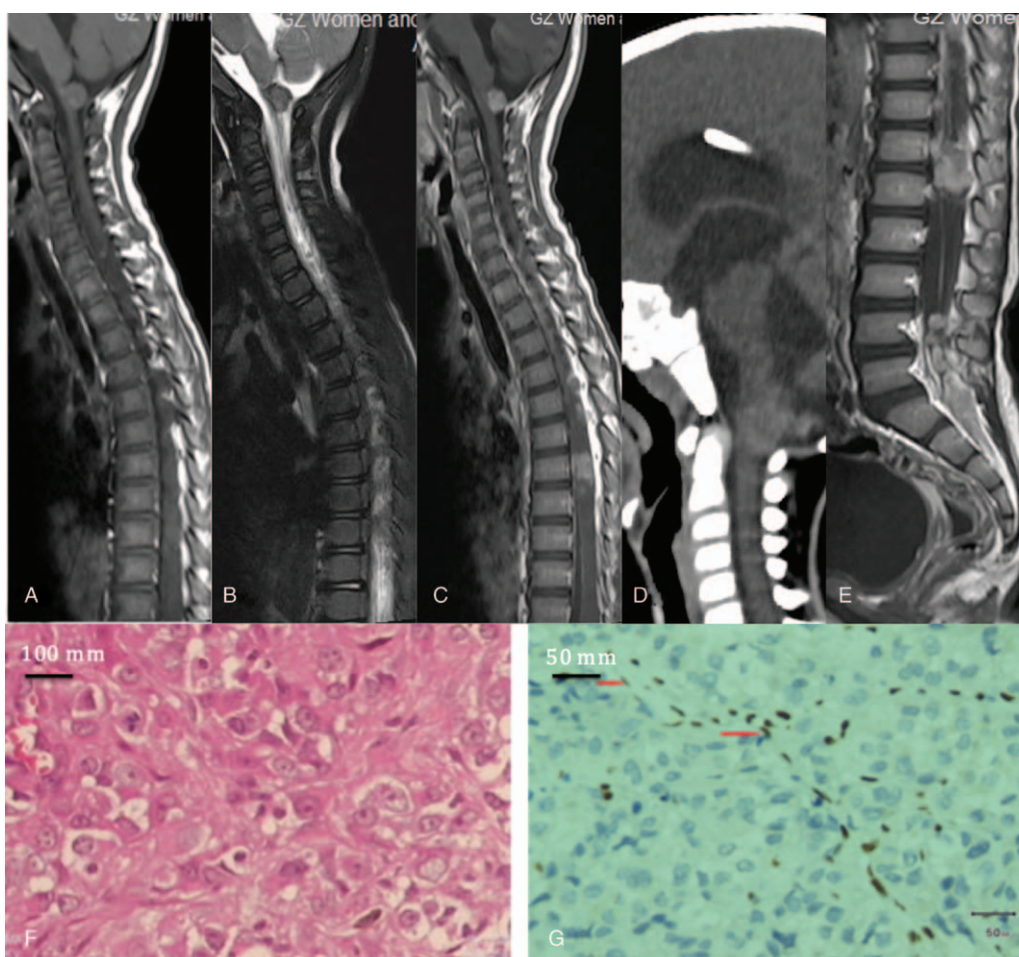


Figure 1. AT/RT in multiple of the cervical and lumbar segments of spinal cord. A: T1WI reveals isointensive signals in the nodules of the lateral cervical medulla. B: T2WI reveals slightly higher signals, hemosiderin ring is observed around it. C: Enhanced MRI scan reveals obvious enhancement, nodular enhancement in the T6–8 segments of spinal cord (white arrow). D: CT reveals slightly higher density (white arrow). E: T11–L1 and the sacrum are fully filled with tumors. Enhanced scan reveals that the spinal meninges are obviously enhanced (arrowhead). Figures F–G: Under the microscope the tumor tissues are varies in shape, the tumor cells are diffused and arranged in pieces, and part of the cells seem like rhabdoid cells. AT/RT=atypical teratoid/rhabdoid tumors, CT=computed tomography, MRI=magnetic resonance imaging.

children, while the tumor affected the subdural space in 1 child. The tumor invaded a wide range of the spinal canal, and mostly affected >3 segments of the spinal cord.

Tumors usually affected the junction of the thoracolumbar spinal cord (7/8, 87.5%). In 1 child, only the lumbar spine was affected and the range of involvement is long. In 7 children, tumors affected >3 segments of the spinal cord, and averagely affected 4.8 segments of the spinal cord. In 1 child, the tumor affected 2 segments of the spinal cord. In 1 child, the lesion presented with skip growth in the neck segment, lower thoracic segment of the spinal cord, and the lumbar and sacral canal (case 2). Total spinal cord metastasis was observed in 1 child (case 5) (Table 1).

3.3. The shape, size, maximum diameter plane, signal (density) and characteristics of the enhanced tumor

3.3.1. Shape and size. Intraspinal tumors in 5 children manifested as nodular (1 child) or long-strip (4 children) masses, and the longest axis of these long strip lesions grew along the vertical axis of the spinal cord. The size of the tumor was 0.4 to 6.0cm, and the maximum diameter was the upper-to-lower diameter, which was significantly larger than the transverse

diameter and anterior-to-posterior diameter (Table 2). Tumors in 3 children were lobulated, which destroyed the ipsilateral intervertebral foramen and affected the sacral canal.

3.3.2. Signal (density) and characteristics of enhancement (including both CT and MRI)

3.3.2.1. Density of Computed tomography. The abdominal and sacrococcygeal tumors exhibited iso-density signals (the CT value was 33 HU and 41 HU, Fig. 2A). The internal density was even, the CT images did not show any sign of bleeding, and the enhanced scan exhibited a mild-to-moderate enhancement (the CT value increased by 8HU/11 HU, Fig. 2B).

One child was negative in the brain CT result (the MRI result was also negative). A slightly higher density nodular shadow could be observed in the lateral side of the medulla oblongata in 1 child (Fig. 1D).

3.3.2.2. Signal of Magnetic resonance imaging. The signals were uneven in the tumors. T1WI mainly presented with iso-density signals (compared with spinal cord signals) in 5 children (Fig. 1A), and mainly presented with slightly high signals in 3 children (Fig. 3A). Furthermore, T2WI mainly presented with

Table 1

Clinical data and prognosis of 8 children with spinal AT/RT.

| Position | Age | Gender | Clinical symptoms | Segments of spinal cord | Aggregated affected segment | Position | Craniocerebral/surrounding condition | Operation condition | Metastasis | Prognosis |
|-------------------------------|-----|--------|---|--|-----------------------------|---------------------------------|--|--|---|---|
| Confined to the spinal column | 3Y | F | Headache for 2 months, pain in bilateral planta and lower limbs and fatigue for 20 days | T10-L1; sacral canal | 4 | Subdural | Hydrocephalus; cisterna magna arachnoid cyst | T10-L1 microscopic total resection of T10-L1 | No | Loss to follow-up |
| | 3Y | F | Headache and vomiting for 3 months (hydrocephalus treatment), sudden adynamia of the lower extremities for 3 days | Medulla oblongata, T6-8; T11-L1; L5 and sacral canal | 6 | Subdural | Hydrocephalus and whole meningeal enhancement; right intervertebral foramen invasion | T11-L1 lesion resection | Medulla oblongata metastasis after 3 months | Loss to follow-up |
| | 3Y | F | Asthenia of the lower limbs for 1 week, cough for 5 days, aggravation complicated with urinary retention for 2 days | T6-T12 | 6 | Epidural | Brain (-) | Microscopic total resection | No | Loss to follow-up |
| | 5Y | F | Pain in lower limbs for 15 days | L3-S1, sacral canal | 4 | Subdural | NA | Microscopic total resection | No | Loss to follow-up |
| | 2Y | M | Asthenia of the lower limbs for 8 days, fever for 3 days | T9-L3 | 6 | Subdural | Hydrocephalus with intracranial and spinal cord diffuse metastasis; right arachnoid cyst | Partial resection, thickening and swelling of nerve root | Brain metastases | Metastasis and recurrence after 1 month |
| Paravertebral | 3Y | M | Right leg pain complicated with claudication for 1 month | L1-3 | 3 | Epidural/paravertebral | Enlargement of intervertebral foramen/paravertebral soft tissue shadow | †Total resection/chemoradiotherapy‡ | No | Recurrent after 1 year |
| | 2Y | M | Asthenia of the lower limbs for 5 days, urinary retention for 1 day | Below T9, sacral canal | 8 | Subdural/paravertebral | Enlargement of intervertebral foramen/paravertebral soft tissue shadow | Almost total resection | No | Loss to follow-up |
| | 3Y | F | Unstable walking, adynamia of the lower limbs with incontinence for 30 days | Below L3, sacral canal | 3 | Epidural/sacroccoccygeal region | Sacral hole, sacral destruction and soft tissue mass | Biopsy | No | Loss to follow-up |

* Mean this patient had carried out MRI in other Hospital 3 months before.

† ICE (ifosfamide + carboplatin + etoposide) + CAV (VP + IFO + CBP vincristine + cyclophosphamide + actinomycin D).

| Position | | Age | Gender | Segments of spinal cord | Position | Size (length* width*height) | Shape | Hemorrhage/ calcification | Enhanced CT | | Imaging findings | | | Immunohistochemistry | | | |
|------------------------------------|--|-----|--------|--|---|--|-------------------|---------------------------|-------------|----------|------------------|-----------------|---|----------------------|----|-----|----------|
| | | | | | | | | | CT | CT | T1WI | T2WI | Tumor enhancement | INI-1 | CK | EMA | Vimentin |
| Confined to CNS | | 3Y | F | T10-L1(4); sacral canal | Subdural space | 1.5*1.5*5.8 | Strip | +/- | NA | NA | Isointensive | Slightly higher | Slight enhancement of tumor and meninges and nerve root | - | NA | + | NA |
| | | 3Y | F | Medulla oblongata, T6-8; T11-L1; L5 and sacral canal | Subdural space | 1.1*1.3*1.0 (medulla oblongata) 0.8*0.6*2.0 (T6-8) 0.8*1.4*2.1 (T8-L1) | Strip and nodular | +/- | 43 | NA | Slightly higher | Slightly lower | Obvious enhancement of tumor and meninges and nerve root | - | + | + | + |
| | | 3Y | F | T6-L2 | Epidural space | 1.2*0.4*10.1 | Strip | +/- | -(Brain) | -(Brain) | Slightly higher | Slightly lower | Slight enhancement of tumor, compression of and enhancement of spinal meninges and nerve root | - | + | + | + |
| | | 5Y | F | L3-S1 sacral canal | Subdural space | 1.5*1.2*2.8 | Strip | +/- | NA | NA | Slightly higher | Slightly higher | Obvious enhancement of tumor and meninges and nerve root | - | + | + | + |
| | | 2Y | M | T9-L3 | Subdural space | 1.4*2.1*11.5 | Strip | Partial +/- | NA | NA | Isointensity | Slightly higher | Obvious enhancement of tumor/ meninges and nerve root | - | + | + | NA |
| Involvement of paravertebral space | | 3Y | M | L1-3 | Epidural space /right paravertebral space | 6.0*2.0*3.2 (upper-to-lower diameter) | Mass | - | 44HU | 52HU | Isointensity | Slightly higher | Obvious enhancement of tumor/ recurrence of enhancement of spinal meninges and nerve root | - | - | + | NA |
| | | 2Y | M | Below T9 | Subdural space /right paravertebral space | 1.6*1.2*14.3 (intraspinal) 2.9*4.1*5.6 (paravertebral) | Mass | +/- | NA | NA | Isointensity | Slightly higher | Slight enhancement of tumor and meninges | - | + | - | NA |
| | | 3Y | F | Below L2 | Epidural space/left sacrococcygeal region | 3.6*5.8*7.6 (sacroiliac) 1.1*2.3*9.1 (intraspinal) | Mass | +/- | 31 | 42 | Isointensity | Slightly higher | Uneven obvious/obvious | - | NA | NA | + |

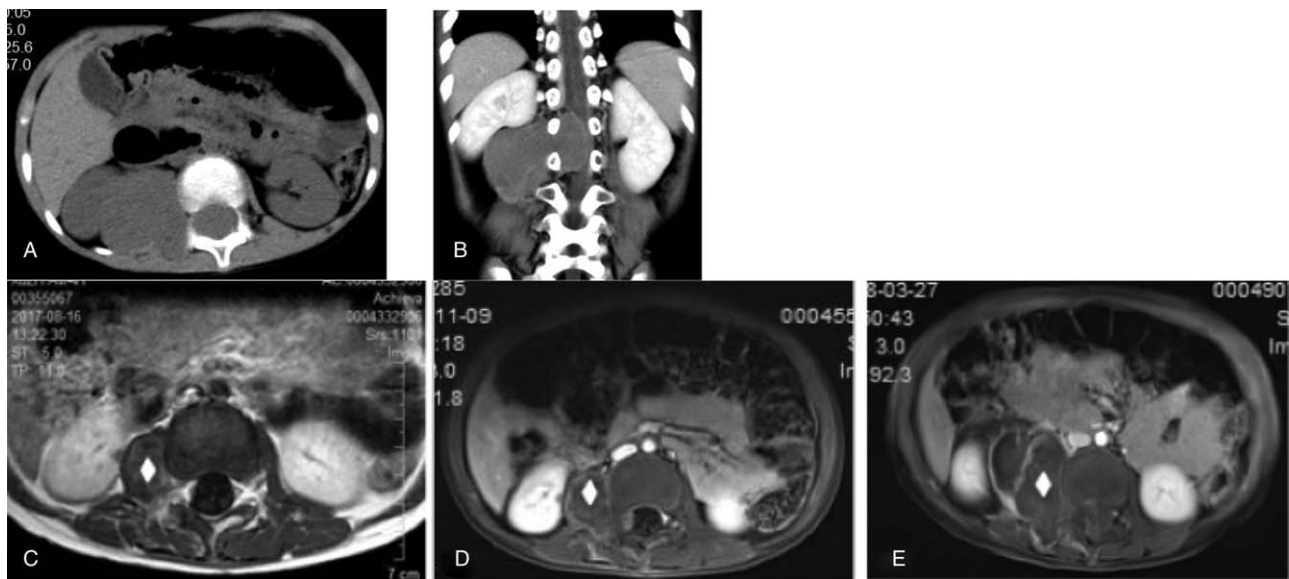


Figure 2. The paravertebral AT/RT affects the spinal canal, which recurs after treatment (surgical resection and radiotherapy). A: Lateral spinal soft tissue mass in right renal hilum, non-enhanced CT scan reveals isointensity. B: Enhanced CT scan coronal image reveals that masses are slightly unevenly enhanced. Masses destroy the intervertebral foramen and affect the epidural space, the spinal cord is obviously compressed. C, D, and E present upper abdominal axial enhanced MRI images at 12 months, 14 months, and 18 months after postoperative chemotherapy (ICE + CAV), respectively, it can be seen that some of masses in the original operation sites gradually grow (white diamond). AT/RT=atypical teratoid/rhabdoid tumors, CT=computed tomography, MRI=magnetic resonance imaging.

slightly higher signals in 6 children (Fig. 3B), and mainly presented with iso-signals in 2 children. Irregular punctiform, linear, and patch-like subacute or obsolete bleeding signals (hemosiderin ring) were found in the tumors and their margins (Fig. 1B).

The enhanced scan revealed that the patterns of tumor enhancement varied: obvious enhancement was found in 4 children (Fig. 1E), while mild to moderate enhancement was found in 4 children (Fig. 3C).

3.4. Intracranial manifestation

Signs of hydrocephalus, such as supratentorial ventricular system dilatation, occurred in 3 children (the enhanced MRI scan revealed no definite metastasis signs, Fig. 3D).

Intracranial scans showed multiple nodules in brain stem and cerebellum, with T2WI higher signals and T1WI lower signals. Intracranial meningeal scan showed intense enhancement in pia mater especially in flair-enhanced imaging.

3.5. Surrounding invasion and metastasis

3.5.1. Surrounding invasion of tumors. Spinal meningeal enhancement around the tumor was observed in 6 children (75%), while 4 children (50%) were complicated with bilateral nerve root enhancement. In 1 child, the tumor grew around the spinal cord, which resulted in swelling of the spinal cord, and presented with uneven signals. In 3 children, the tumors destroyed the intervertebral foramen and grew in the sacral foramen (Fig. 2B), forming soft tissue masses in the paravertebral tissues and hips.

3.5.2. Sacral invasion. When the primary tumor was not contiguous to the sacral tumor, we defined as sacral invasion. Five children showed sacral invasion. In 2 children, since the tumors invaded/located in the sacrococcygeal region, it could not be distinguished whether the tumor was derived from invasion or

metastasis. In 3 children, the manifestations were that the tumors filled the sacral canal (Fig. 3C), thickening/swelling of the cauda equina (Fig. 1E), or blood accumulation in the sacral canal occurred, and the nerve of the cauda equina was mostly unclear.

3.6. Tumor metastasis and recurrence

The tumor recurred in 1 child at 1 year after the operation (Fig. 2C–E). Furthermore, the tumor recurred and craniocerebral metastasis occurred in 1 child at 1 month after the operation (Fig. 4A–C). The sizes of these recurrent and metastatic tumors were significantly larger than those of the primary lesions. The remaining 6 children were lost to follow-up at 3 months after operation.

3.7. Pathological manifestations

The tumor masses were roughly fish flesh-, jelly-, or tofu jelly-like, and all presented with bleeding. Under a microscope, the tumor cells had various morphologies and were densely distributed, and obvious hemorrhagic necrotizing and striated muscle-like cells could be observed (Fig. 1F–G).

Immunohistochemistry: Anti-oncogene integrase interactor 1 (INI-1) was negative in 8 children (Fig. 3E). Vimentin was positive in 4 children. Glial fibrillary acidic protein (GFAP) was positive or focally positive in 6 children. The expression of cell proliferation marker (Ki-67) was 30% to 80% in 7 children, and <5% in 1 child. Acidic calcium binding protein 100 (S-100) was positive or partially positive in 6 children. Epithelial membrane antigen (EMA) was positive or partially positive in 5 children (Table 2).

4. Discussion

Malignant rhabdoid tumor (RT) is a rare invasive tumor with high malignancy, which mainly occurs in infants and young

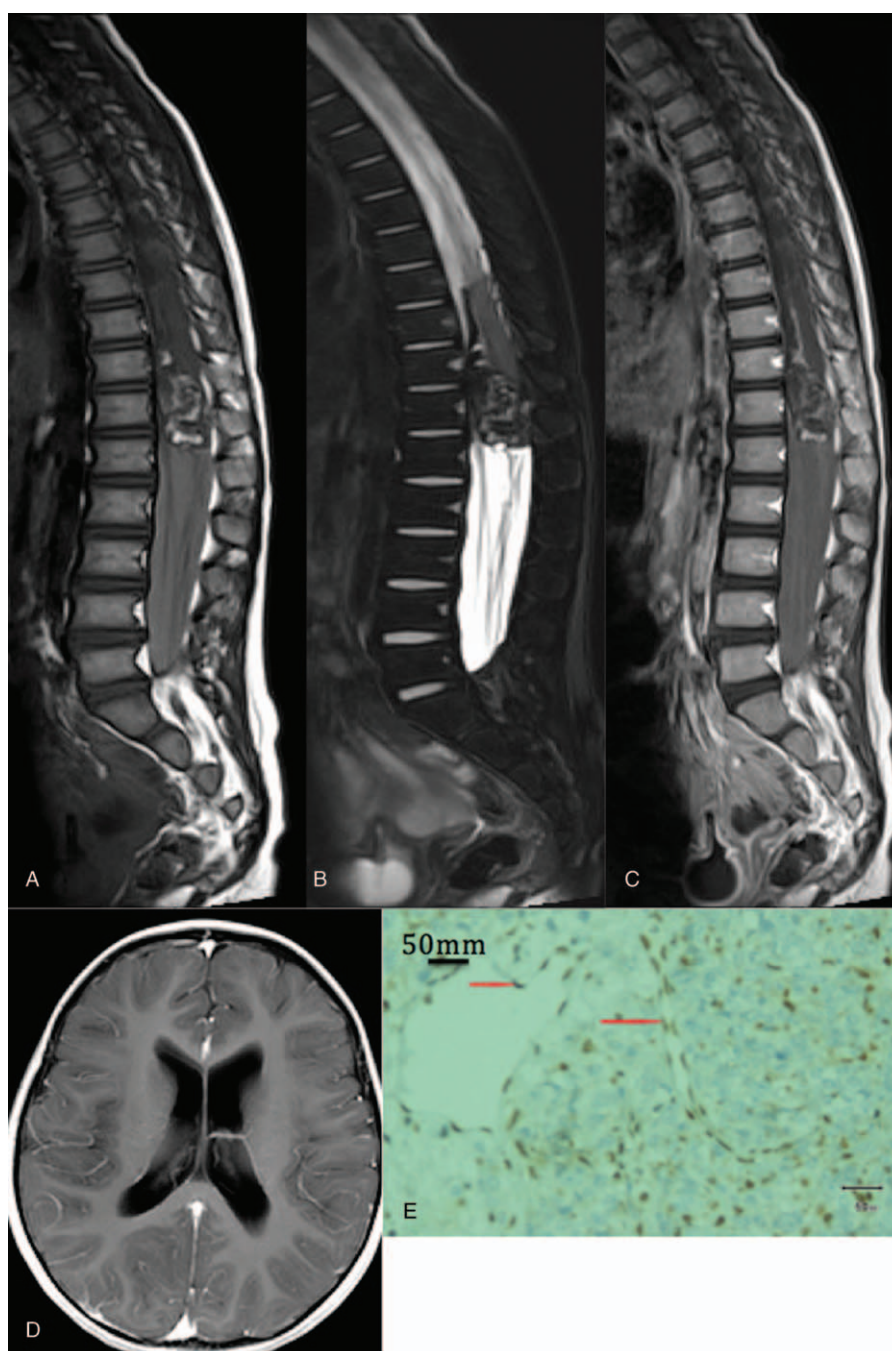


Figure 3. T10-L1 vertebral AT/RT and supratentorial cerebral ventricular system dilation. A: Sagittal T1WI reveals that the T10-L1 vertebrae present with horizontal and oval space occupying, T1WI reveals mixed slightly higher signals, patchy, and striped bleeding (white triangle) are observed. The sacral canal is fully filled with soft tissue shadows (white star). B: Sagittal T2WI reveals that lesions present with mixed slightly higher signals. C: Sagittal enhanced scanning reveals that, the tumor is slightly enhanced, linear enhancement (white arrow) can be observed in the spinal meninges. D: Head enhanced MRI reveals that, bilateral lateral ventricles are dilated. E: Immunohistochemical staining for INI-1 reveals that, the expression of INI-1 is positive in the nucleus of the vascular endothelial cells in the tumor (red pointer), and negative in the nucleus of surrounding tumor cells. AT/RT=atypical teratoid/rhabdoid tumors, MRI=magnetic resonance imaging.

children. According to the anatomic site of the tumor, RT can be roughly divided into the 3 types: malignant rhabdoid tumor of the kidney (MRTK), atypical teratoid/rhabdoid tumor (AT/RT), in the central nervous system (CNS), and extrarenal extracranial rhabdoid tumor (EERT).^[18] Although spinal AT/RT is a rare tumor in children, based on what we find in the present study, we can diagnose correctly or at least not miss it before surgery.

4.1. Epidemiology and clinical manifestations

AT/RT is the most common CNS malignant tumor in children <3 years old,^[19,20] which accounts for 2% to 3% of all children with brain tumors,^[21] and 17.3% of all children with malignant brain tumors. This tumor was first defined by Rorke et al^[22] in 1996, and was classified as embryonal tumor of the CNS by the World Health Organization (WHO) in 2016. The predilection sites of

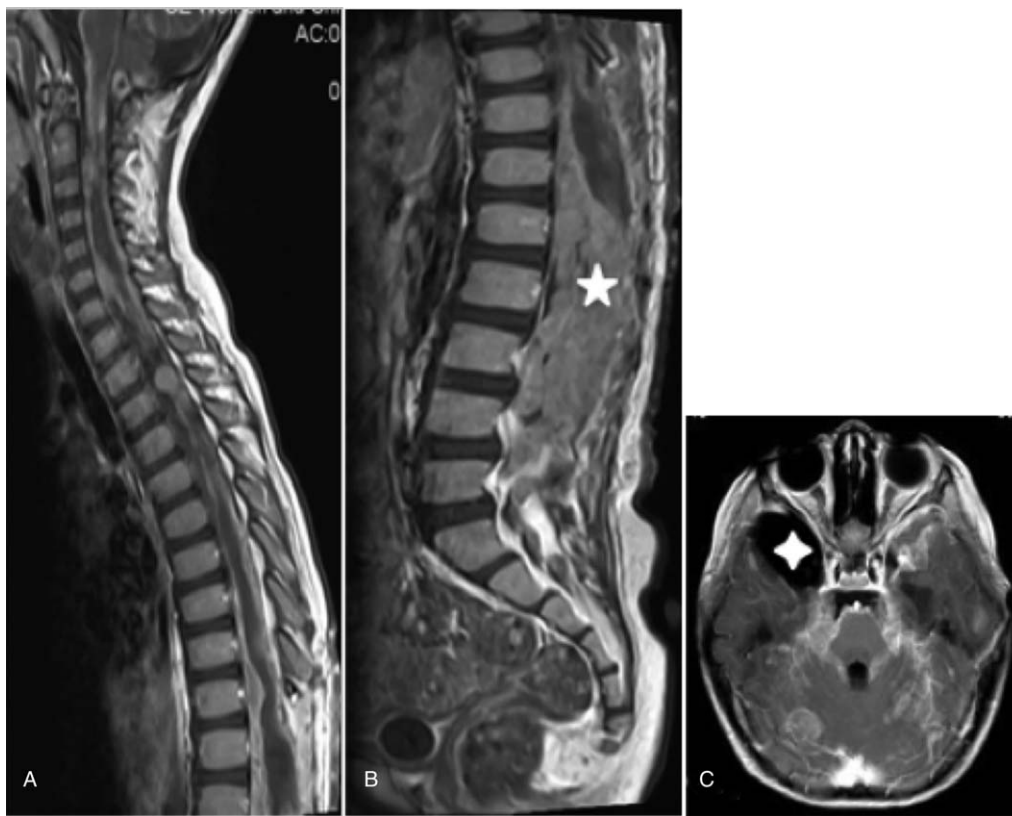


Figure 4. Spinal AT/RT with whole spinal cord and whole brain diffuse metastases. A: Sagittal enhanced MRI scan reveals obvious diffuse nodular enhancement of the cervical and thoracic spinal cord. B: Enhanced scan reveals that tumors are fully filled in the sacral canal and are obviously enhanced. C: Craniocerebral axial enhanced scan reveals diffuse thickening and obvious enhancement of the meninges, nodular metastases of the right cerebellar hemisphere, and right temporal arachnoid cyst (white single diamond). AT/RT=atypical teratoid/rhabdoid tumors, MRI=magnetic resonance imaging.

CNS AT/RT are usually located in different parts of the body, between adult and child.^[23] In children, it commonly occurs in the posterior cranial fossa (61%), followed by the cerebral hemisphere (20%), the third ventricle and sella turcica (5%), the pineal region (5%), and spine (1%).^[31] These tumors can invade the cranium or directly invade towards the outer cranium.^[24–29] However, AT/RT rarely occurs in the spine.^[30,31] In our hospital, 31 patients with CNS AT/RT confirmed by surgical pathology were diagnosed in the same period: The tumor occurred in the posterior cranial fossa in 14 children (45.2%), in the cerebral hemisphere in 5 children (16.1%), in the intracranial pineal region (12.9%) in 4 children (12.9%), and in the spine in 8 children (25.8%). The incidence of AT/RT in the spine is similar to that in the cerebral hemisphere and pineal region, which is higher than that reported in a literature.^[31]

Behdad and Perry^[32] considered that the incidence was slightly higher in boys than in girls.^[33] In the present study, the number of girls were slightly more than the number of boys. These were not consistent with those reported in literature.^[31] It was speculated that the reason may be that these literatures commonly focused on the clinical characteristics of craniocerebral AT/RT, and all data in the present study pertained to spinal AT/RT, causing the incidence of the disease and proportion of sex to be different to a certain extent. Sinha et al^[34] was the first to report that adult spinal AT/RT can be characterized by cauda equina syndrome. In present study it was consistent with that reported in literatures. Indeed, all lesions in the cauda equina and metastasis or invasion of cauda equina presented with the cauda equina syndrome. It is

noteworthy that when children only presented with a headache, spinal lesions may be missed, causing loss of the best time for treatment. In the present study, 2 children underwent head enhanced MRI due to headache at 3 months prior. The result only revealed a ventriculo system dilatation, and the sign of metastasis of the whole brain and whole spinal cord was found in 1 child at reexamination. This phenomenon needs to be given more attention in the future. If a child develops a headache without other incentives, while the head MRI reveals hydrocephalus or meningeal enhancement, the possibility of spinal AT/RT should be alerted, and an enhanced MRI scan of the whole spine should be performed as early as possible.

AT/RT is very invasive and grows rapidly, and the 5-year survival rate is only 33%.^[35] The main causes of death are tumor recurrence or leptomeningeal dissemination (LMD). The median survival period is 21 months in adults, and decreases to 6.00 to 16.75 months in children.^[19,22,36] The recurrence and metastasis rates were consistent with that reported in a literature by Madigan et al.^[37]

4.2. Pathological changes

Histologically, AT/RT can consist of striated muscle-like cells (13%), as well as pre-existing cell neurological epithelium (67%), mesenchymal tissue (31%), or epithelial tissue (25%).^[38,39]

The immunohistochemical manifestations of AT/RT also vary. A study revealed that AT/RT is correlated to the mutation or deletion of tumor suppressor gene INI-1, which can be used to

distinguish it from other embryonal tumors. Immunohistochemistry combined with INI-1 protein expression deletion is the gold standard for diagnosing AT/RT.^[40–44] In addition, AT/RT can be positive for vimentin, EMA, SMA, synaptophysin, CD99, GFAP, S-100, and cytokeratin.

In the present study, in all children, striated muscle-like cells were found by microscopy, and the protein expression of INI-1 was absent. Among these children, intraspinal tumors and immunohistochemical indexes were basically consistent with the AT/RT diagnosis in 5 children.^[45] Vimentin was not detected in 3 children with involvement of the internal and external vertebral canal, and the remaining characteristics were also consistent with the diagnosis of malignant RT.

4.3. Imaging findings

In the present study, the images of the spinal AT/RT were mainly classified into 2 types: one type is that tumors are confined in the spinal column, that is, the typical CNS AT/TR, accounting for 62.5%; the other type is that tumors affect the paravertebral tissues, accounting for 37.5%. Spinal AT/RT usually occurs at the junction of the thoracolumbar spinal cord. Tumors were located in the subdural space in 5 children, and in epidural space in 3 children, which was consistent with that reported in a literature.^[46] The tumor grows along the longitudinal axis of the spinal cord, in which the upper-to-lower diameter is significantly longer than the anterior-to-posterior diameter and right-to-left diameter of the tumor, and >3 vertebral segments were affected.

On the MRI images, the tumors exhibited mixed signals on T1WI and T2WI images. T2WI images exhibited slightly higher/iso-density signals, while T1WI images exhibited an iso-density/slightly high signal, which was consistent with that reported in literatures.^[47,48] The results of the present study revealed that spinal AT/RT was very likely to induce bleeding (100%).^[7,49] The investigators consider that this is one of the typical signs of spinal AT/RT, and that the patterns of tumor enhancement vary. The data in the present study revealed that 62.5% of spinal AT/RT affected the sacral canal, 75% of the spinal AT/RT exhibited spinal meningeal enhancement, and 50% of the spinal AT/RT exhibited nerve root enhancement. It was speculated that the reason may be that AT/RT has a high degree of malignancy, which easily causes cerebrospinal fluid metastases or bleeding in tumor, and the falling off of tumor cells. This is also the cause that AT/RT are characterized by cauda equina syndrome. It is noteworthy that in 4 children with obviously enhanced tumors, recurrence and metastasis occurred in 2 children after the operation, and occurred in the paraspinal soft tissue in 2 children after the operation. It remains to be determined whether a consistency exists among the degree of tumor enhancement, tumor recurrence, and the surrounding invasion. The mass wrapped around the spinal cord in 1 child resulted in swelling of the spinal cord, and the T2WI signals were elevated.

On the CT images, the masses mostly exhibited an iso-density/slightly higher density (paraspinal and sacrococcygeal), which may be consistent with the composition of striated muscle-like cells. Furthermore, the enhanced CT scan revealed mild-to-moderate enhancement. No CT sign of bleeding in the tumor was found. The reason may be that the density resolution of CT was low, or bleeding in the tumor was at the non-acute phase.

4.4. Differential diagnosis

The extramedullary subdural tumors in children are mostly neurogenic tumors (schwannoma and neurofibroma) and

meningioma. Bleeding did not easily appear in the tumor, and growth along spinal cord vertical axis and spinal meningeal nerve root metastasis are rare. Epidural tumors in children are mostly metastatic tumors, such as neuroblastoma, primitive neuroectodermal tumor (PNET), and Ewing sarcoma. Calcification easily occurs in neuroblastoma, but the signs of spinal meningeal metastasis and nerve root enhancement are rare. The bone destruction of PNET and Ewing sarcoma is obvious, masses in the paravertebral soft tissue are generally large, and necrosis is more obvious than bleeding. Angiogenic lesions in the spinal cord: arteriovenous teratoblastoma and congenital hemangioma can grow along the vertical axis of the spinal cord, the spinal cord is mostly characterized by ischemic changes, and the typical manifestation is a multiple snake-like flowing-void sign (AVM) or obvious T2WI high signal (hemangioma), which can be significantly enhanced after enhancement. Furthermore, spinal meningeal and nerve root enhancement are rare.

4.5. Limitations and prospective

In the present study, the sample size was small and it is a retrospective cohort study. Most of the children left the hospital after surgery or biopsy, and went back hometown for treatment, so loss of follow-up is also a deficiency of this study.

There is no final conclusion on whether paraspinal and sacrococcygeal tumors that invade the spinal canal should be classified as spinal AT/RT. However, the imaging findings, clinical manifestations, and therapies of AT/RT in the internal and external vertebral canal were similar to those of intraspinal AT/RT, which can be combined for discussion. Furthermore, 1 child was normal before the operation in the craniocerebral non-enhanced CT, while 1 child presented with meningeal enhancement at 3 months after head craniocerebral MRI. However, it could not be temporarily determined whether the missing primary intracranial lesions were missed. Finally, the lesions in 1 child were multiple spinal segment lesions, the lesion in the cervical spinal cord was not observed in the head CT before the operation, and cervical and thoracolumbar lesions occurred 3 months later. It remains to be determined whether thoracolumbar lesion is a primary lesion.

In summary, extramedullary tumors in 2 to 5-year-old children are clinically characterized by cauda equina syndrome, and MRI suggests multiple segmental involvement at the thoracolumbar junction. When the tumor grows along the vertical axis of the spinal cord and bleeding occurs in the tumor, the possibility of spinal AT/RT should be highly considered. Biopsy combined with immunohistochemistry is the gold standard for its diagnosis. When it is suspected to be CNS AT/RT, craniocerebral and whole spinal column enhanced MRI should be routinely performed.

Author contributions

Conceptualization: Lian-Wei Lu, He-Hong Li, Jin-Sheng Tian.

Data curation: Lian-Wei Lu, He-Hong Li, Jin-Sheng Tian.

Investigation: Lian-Wei Lu, He-Hong Li, Jin-Sheng Tian.

Methodology: Jian-Ming Li, Zheng-Rong Chen.

Project administration: Wen-Biao Xu.

Resources: Jian-Ming Li, Zheng-Rong Chen.

Software: Jian-Ming Li, Zheng-Rong Chen.

Supervision: Wen-Biao Xu.

Validation: Wen-Biao Xu.

Writing – original draft: Hui-Ying Wu.

Writing – review & editing: Hui-Ying Wu.

References

- [1] Ginn KF, Gajjar A. Atypical teratoid rhabdoid tumor: current therapy and future directions. *Front Oncol* 2012;2:114.
- [2] Tulla M, Berthold F, Graf N, et al. Incidence, trends, and survival of children with embryonal tumors. *Pediatrics* 2015;136:e623–32.
- [3] Ostrom QT, Chen Y, M de Blank P, et al. The descriptive epidemiology of atypical teratoid/rhabdoid tumors in the United States, 2001–2010. *Neuro Oncol* 2014;16:1392–9.
- [4] Meyers SP, Khademan ZP, Biegel JA, et al. Primary intracranial atypical teratoid/rhabdoid tumors of infancy and childhood: MRI features and patient outcomes. *AJNR Am J Neuroradiol* 2006;27:962–71.
- [5] Ud Din N, Barakzai A, Memon A, et al. Atypical teratoid/rhabdoid tumor of brain: a clinicopathologic study of eleven patients and review of literature. *Asian Pac J Cancer Prev* 2007;18:949–54.
- [6] Liebigt S, Florschütz A, Arndt N, et al. Atypical teratoid/rhabdoid tumor of the pineal region in a young adult male patient: case report and review of the literature. *J Neurol Surg A Cent Eur Neurosurg* 2017;78:92–8.
- [7] Jin B, Feng XY. MRI features of atypical teratoid/rhabdoid tumors in children. *Pediatr Radiol* 2013;43:1001–8.
- [8] Judkins AR, Burger PC, Hamilton RL, et al. INI1 protein expression distinguishes atypical teratoid/rhabdoid tumor from choroid plexus carcinoma. *J Neuropathol Exp Neurol* 2005;64:391–7.
- [9] Judkins AR, Mauger J, Ht A, et al. Immunohistochemical analysis of hSNF5/INI1 in pediatric CNS neoplasms. *Am J Surg Pathol* 2004;28:644–50.
- [10] Chen ML, McComb JG, Krieger MD. Atypical teratoid/rhabdoid tumors of the central nervous system: management and outcomes. *Neurosurg Focus* 2005;18:E8.
- [11] Strother D. Atypical teratoid rhabdoid tumors of childhood: diagnosis, treatment and challenges. *Expert Rev Anticancer Ther* 2005;5:907–15.
- [12] Richardson EA, Ho B, Huang A. Atypical teratoid rhabdoid tumour: from tumours to therapies. *J Korean Neurosurg Soc* 2018;61:302–11.
- [13] Dufour C, Beaugrand A, Le Deley MC, et al. Clinicopathologic prognostic factors in childhood atypical teratoid and rhabdoid tumor of the central nervous system: a multicenter study. *Cancer* 2012;118:3812–21.
- [14] von Hoff K, Hinkes B, Dannemann-Stern E, et al. Frequency, risk-factors and survival of children with atypical teratoid rhabdoid tumors (AT/RT) of the CNS diagnosed between 1988 and 2004, and registered to the German HIT database. *Pediatr Blood Cancer* 2011;57:978–85.
- [15] Xin X, Zhu B, Shen J, et al. A primary spinal extradural atypical teratoid/rhabdoid tumor of the cervical spine with bony involvement. *J Child Neurol* 2014;29:670–3.
- [16] Chao MF, Su YF, Jaw TS, et al. Atypical teratoid/rhabdoid tumor of lumbar spine in a toddler child. *Spinal Cord Ser Cases* 2017;3:16026.
- [17] Bannykh S, Duncan C, Ogle E, et al. Atypical teratoid/rhabdoid tumor of the spinal canal. *J Neurooncol* 2006;76:129–30.
- [18] Uwineza A, Gill H, Buckley P, et al. Rhabdoid tumor: the Irish experience. *Cancer Genet* 2014;207:398–402.
- [19] Hilden JM, Meerbaum S, Burger P, et al. Central nervous system atypical teratoid/rhabdoid tumor: results of therapy in children enrolled in a registry. *J Clin Oncol* 2004;22:2877–84.
- [20] Woehrer A, Slavic I, Waldhoer T, et al. Austrian Brain Tumor Registry Incidence of atypical teratoid/rhabdoid tumors in children: a population-based study by the Austrian Brain Tumor Registry. *Cancer* 2010;116:5725–32.
- [21] Coccé MC, Lubieniecki F, Kordes U, et al. A complex karyotype in an atypical teratoid/rhabdoid tumor: case report and review of the literature. *J Neurooncol* 2011;104:375–80.
- [22] Rorke LB, Packer RJ, Biegel JA. Central nervous system atypical teratoid/rhabdoid tumors of infancy and childhood: definition of an entity. *J Neurosurg* 1996;85:56–65.
- [23] Lafay-Cousin L, Hawkins C, Carret AS, et al. Central nervous system atypical teratoid rhabdoid tumours: the Canadian Paediatric Brain Tumour Consortium experience. *Eur J Cancer* 2012;48:353–9.
- [24] Oka H, Scheithauer BW. Clinicopathological characteristics of atypical teratoid/rhabdoid tumor. *Neurol Med Chir (Tokyo)* 1999;39:510–7.
- [25] Robbins C, Vanwyck R, Wilms G, et al. An extrarenal rhabdoid tumor of the cervical spine with bony involvement. *Skeletal Radiol* 2007;36:341–5.
- [26] Evans A, Ganatra R, Morris SJ. Imaging features of primary malignant rhabdoid tumour of the brain. *Pediatr Radiol* 2001;31:631–3.
- [27] Robson DB, Akbarnia BA, deMello D, et al. Malignant rhabdoid tumor of the thoracic spine. Case report. *Spine (Phila Pa 1976)* 1987;12:620–4.
- [28] Balaton AJ, Vaury P, Videgrain M. Paravertebral malignant rhabdoid tumor in an adult. A case report with immunocytochemical study. *Pathol Res Pract* 1987;182:713–8.
- [29] Lynch HT, Shurin SB, Dahms BB, et al. Paravertebral malignant rhabdoid tumor in infancy. In vitro studies of a familial tumor. *Cancer* 1983;52:290–6.
- [30] Tamiya T, Nakashima H, Ono Y, et al. Spinal atypical teratoid/rhabdoid tumor in an infant. *Pediatr Neurosurg* 2000;32:145–9.
- [31] Tanizaki Y, Oka H, Utsuki S, et al. Atypical teratoid/rhabdoid tumor arising from the spinal cord—case report and review of the literature. *Clin Neuropathol* 2006;25:81–5.
- [32] Behdad A, Perry A. Central nervous system primitive neuroectodermal tumors: a clinicopathologic and genetic study of 33 cases. *Brain Pathol* 2010;20:441–50.
- [33] Warmuth-Metz M, Bison B, Dannemann-Stern E, et al. CT and MR imaging in atypical teratoid/rhabdoid tumors of the central nervous system. *Neuroradiology* 2008;50:447–52.
- [34] Sinha P, Ahmad M, Varghese A, et al. Atypical teratoid rhabdoid tumour of the spine: report of a case and literature review. *Eur Spine J* 2015;24 (suppl 4):S472–84.
- [35] Asada N, Kato I, Daifu T, et al. Good response to chemotherapy spares irradiation for extrarenal rhabdoid tumor conferring better activities of daily living. *J Pediatr Hematol Oncol* 2015;37:e57–9.
- [36] Samaras V, Stamatelli A, Samaras E, et al. Atypical teratoid/rhabdoid tumor of the central nervous system in an 18-year-old patient. *Clin Neuropathol* 2009;28:1–0.
- [37] Madigan CE, Armenian SH, Malogolowkin MH, et al. Extracranial malignant rhabdoid tumors in childhood: the Childrens Hospital Los Angeles experience. *Cancer* 2007;110:2061–6.
- [38] Schrey D, Carceller Lechón F, Malietz G, et al. Multimodal therapy in children and adolescents with newly diagnosed atypical teratoid rhabdoid tumor: individual pooled data analysis and review of the literature. *J Neurooncol* 2016;126:81–90.
- [39] Rumboldt Z, Camacho DL, Lake D, et al. Apparent diffusion coefficients for differentiation of cerebellar tumors in children. *AJNR Am J Neuroradiol* 2006;27:1362–9.
- [40] Kohashi K, Oda Y, Yamamoto H, et al. SMARCB1/INI1 protein expression in round cell soft tissue sarcomas associated with chromosomal translocations involving EWS: a special reference to SMARCB1/INI1 negative variant extraskeletal myxoid chondrosarcoma. *Am J Surg Pathol* 2008;32:1168–74.
- [41] Bourdeaut Z, Fréneaux P, Thuille B, et al. Extra-renal non-cerebral rhabdoid tumours. *Pediatr Blood Cancer* 2008;51:363–8.
- [42] Yuri T, Danbara N, Shikata N, et al. Malignant rhabdoid tumor of the liver: case report and literature review. *Pathol Int* 2004;54:623–9.
- [43] Hoot AC, Russo P, Judkins AR, et al. Immunohistochemical analysis of hSNF5/INI1 distinguishes renal and extra-renal malignant rhabdoid tumors from other pediatric soft tissue tumors. *Am J Surg Pathol* 2004;28:1485–91.
- [44] Rosty C, Peter M, Zucman J, et al. Cytogenetic and molecular analysis of a t(1;22)(p36;q11.2) in a rhabdoid tumor with a putative homozygous deletion of chromosome 22. *Genes Chromosomes Cancer* 1998;21:82–9.
- [45] Russo P, Biegel JA. SMARCB1/INI1 alterations and hepatoblastoma: another extrarenal rhabdoid tumor revealed? *Pediatr Blood Cancer* 2009;52:312–3.
- [46] Kodama H, Maeda M, Imai H, et al. MRI of primary spinal atypical teratoid/rhabdoid tumor: a case report and literature review. *J Neurooncol* 2007;84:213–6.
- [47] Caldemeyer KS, Smith RR, Azzarelli B, et al. Primary central nervous system malignant rhabdoid tumor: CT and MR appearance simulates a primitive neuroectodermal tumor. *Pediatr Neurosurg* 1994;21:232–6.
- [48] Howlett DC, King AP, Jarosz JM, et al. Imaging and pathological features of primary malignant rhabdoid tumours of the brain and spine. *Neuroradiology* 1997;39:719–23.
- [49] Wang H, Ma Y, Li J, et al. [Extrarenal malignant rhabdoid tumor of childhood: a clinicopathologic analysis of 8 cases]. *Zhonghua Bing Li Xue Za Zhi* 2014;43:805–8.